Physicochem. Probl. Miner. Process., 60(2), 2024, 188154

http://www.journalssystem.com/ppmp

Physicochemical Problems of Mineral Processing

ISSN 1643-1049

A case study on the recovery of unevenly embedded particle size in high-carbon chalcopyrite using an alkyne-based thioester collector: Flotation processing and adsorption mechanism

Yuechao Qi [1], Yunbo Luo [2,3], Xianyang Qiu [3], Dezhou Wei [1], Faming Zhang [2,3], Chenghang Wang [3]

[1] Northeastern University, Shenyang 110819, Liaoning, China

[2] Guangzhou Yueyouyan Mineral Resources Technology Co., Ltd, Guangzhou 510651, Guangdong, China

[3] Institute of Resource Utilization and Rare Earth Development, Guangdong Academy of Sciences, Guangzhou 510651, Guangdong, China

Corresponding author: luoyunbo19871114@126.com (Yunbo Luo)

Abstract: The difference in chalcopyrite's primary ore-hosting rocks (dolomite and carbonaceous slate) in the Democratic Republic of the Congo results in an extremely uneven grain size distribution. Additionally, the presence of 2.21% organic carbon in the gangue impacts flotation efficiency. To address these challenges, ore properties were analyzed using the Mineral Liberation Analyzer (MLA), X-Ray Diffractometer (XRD), and microscopy. Flotation process was modified to incorporate a "middlings regrinding" processing, utilizing PDEC (an alkyne-based thioester collector, prop-2-yn-1-yl diethylcarbamodithioate) as the collector for experimental studies. Density Functional Theory (DFT) calculations elucidated the interaction mechanism of PDEC on chalcopyrite's surface. The MLA analysis indicates that chalcopyrite is mainly found in medium to fine grains, with the presence of fine-grained copper minerals smaller than 0.04mm accounting for 16.29% of the sample. This implies that these minerals require fine grinding for effective separation. Despite interference from organic carbon, PDEC demonstrates remarkable selectivity and efficiency in chalcopyrite flotation. By employing the "middlings regrinding" flotation method, a concentrate with a Cu content of 26.79% and a recovery of 87.88% was achieved, representing an increase of 0.17% in Cu grade and 4.09% in recovery rate compared to the conventional flotation process. DFT analysis demonstrates that the S 3p orbitals in carbon-sulfur double bond of PDEC and the C 2p orbitals in its acetylene group significantly affect its collection efficiency, engaging in hybridization with the Fe 3d orbitals on the surface of chalcopyrite, thereby facilitating a robust bonding interaction.

***Keywords*:** chalcopyrite, middlings regrinding, flotation, organic carbon, thioester collectors

1. Introduction

Copper, a cornerstone metal in contemporary industry, plays a pivotal role in power systems, transportation, construction, and a wide array of industrial applications (Zhang et al., 2015). The global distribution of copper ore reveals that approximately 880 million tons of copper resources have been identified worldwide (Wang et al., 2023; Singer, 2017)). Nevertheless, the relentless advancement of society and the economy has led to extensive mining and consumption of mineral resources. Consequently, the availability of high-grade, high-quality, and easily extractable minerals is swiftly declining (Kuipers et al., 2018). The efficient utilization of low-grade ores, characterized by fine grain sizes and intricate structural compositions, presents a formidable challenge (Mudd and Jowitt, 2018; Feng et al., 2022).

Copper ore separation predominantly depends on flotation (Taheri et al., 2014). Insufficient monomer dissociation from coarse grinding results in the retention of finely embedded copper minerals in the middlings throughout the flotation process (Štribanović et al., 2020). Fine grinding is imperative for ores with small grain sizes and complex structures to ensure adequate monomer dissociation. Stirred milling technology, alongside novel ultra-fine grinding techniques, demonstrates significant promise in

DOI: 10.37190/ppmp/188154

mineral processing (Parker et al., 2015). Eswaraiah et al. (2015) evaluated various agitator designs in a stirred mill to achieve an 80% pass rate for magnetite at 38μm, results indicated that the double helical screw agitator design was both more efficient and energy-saving. Hassall et al. (2016) study highlighted that ceramic bead type and size in ultrafine mills are crucial for achieving desired grinding outcomes. Following the fine grinding of Nickel-Copper-PGE mineral, the majority of ceramic beads, maintaining their spherical shape without considerable breakage and fell within the 2.5 to 3.15 mm range, enhancing the copper grade in the concentrate during subsequent sorting. Zhu et al. (2019) introduced an innovative ultra-fine grinding machine based on ball milling theory, achieving efficient material grinding to under 5 μm in just 15 minutes with 95% efficiency. However, these technologies encounter several challenges, including scalability, cost-efficiency, and raw material compatibility. Consequently, treating middlings separately emerges as a viable beneficiation approach (Qiu et al., 2015). Peng et al. (2017) found that gangue minerals encapsulated the residual graphite particles in the middlings from graphite ore flotation in Nanjiang, Sichuan. Concentrating and regrinding the middlings twice led to a roughly 40% increase in graphite concentrate recovery. Wan et al. (2022) explored methods to enhance magnetic separation efficiency for flash-roasted products from LGRIT. Regrinding the middlings reduced the size of magnetic iron particles and their magnetic induction strength, indicating that a high magnetic field strength facilitated the recovery of fine-grained magnetic iron. The optimized process improved the magnetic separation recovery rate by 9%. In Songzi's tantalum-niobium ore, minerals sized -0.040 mm, mainly tantalum-niobium, intermingled with mica, illite, and quartz, and partially coexisted with topaz and zircon, were difficult to liberate individually, Yuan et al. (2015) developed a process flow involving grading, heavy selection, magnetic selection, middlings regrinding, and heavy selection, yielding satisfactory results. Whiteman et al. (2016) applied a regrinding process to separate fine-grained copper from coarse particles in Kamoa copper ore, enhancing copper recovery and achieving a concentrate grade exceeding 28%, thus lowering smelting costs.

Traditional collectors exhibit limited efficacy and selectivity in processing fine particles and complex minerals (Roy et al., 2015; Albrecht et al., 2016). In response, research focusing on environmental sustainability and cost-effectiveness has become increasingly important in the development of copper collectors (Azizi, 2014). Extensive optimization studies by mineral processing researchers have led to the creation of a diverse array of novel reagents (Zhao et al., 2023). Jiang et al., (2014) identified Sodium Isoamylxanthate as the most effective collector for copper mines in Sichuan Province, attaining a copper concentrate grade of 19.09% and a recovery rate of 82.65% under optimal conditions. Atashi and Ebrahimian (2014) found that the A3477 collector was highly effective for copper flotation and pyrite suppression in Middle Eastern copper ores containing sulfide minerals like chalcopyrite and bornite. Ma et al. (2022) study artificial mixed-mineral experiments demonstrated that Ethyl Isobutyl Xanthogenic Acetate (EIBXAC) enhances the copper concentrate's grade without affecting its recovery rate, offering greater efficiency and selectivity. Ryaboy and Shepeta's (2021) investigated the flotation of copper-arsenic ores and highlighted the selectivity of a dialkyl dithiophosphate-type collector in enhancing the recovery of copper, gold, and silver, while also reducing arsenic levels. Additionally, research by Sokolović et al. (2019) on the Majdanpek copper mine's mineralogy and flotation revealed that a mixed collector, comprising isopropyl xanthate, dialkyl dithiophosphate, and SKIKBZ 2000, yielded the best results in terms of copper recovery rate and concentrate grade.

This work focuses on exploring the intricate properties of chalcopyrite from the DRC (Democratic Republic of the Congo), tackling two significant challenges: the highly irregular grain size distribution of chalcopyrite and the influence of organic carbon in the ore on the flotation process. An initial process mineralogical analysis of the chalcopyrite was undertaken. Subsequently, based on these findings, the "middlings regrinding" flotation method and an innovative thioester collector, PDEC, were utilized to improve the recovery of fine-grained copper. The mechanism of interaction between PDEC and chalcopyrite surface was clarified by examining changes in state density. The aim of this work is to enhance flotation techniques for complex, fine-grained copper ores, offer insights into the development of copper collectors, and contribute to the sustainable exploitation of copper ore resources.

2. Materials and methods

2.1. Materials

The sample, sourced from the Democratic Republic of the Congo, was subjected to crushing, grinding,

screening, and drying processes. Table 1 displays the multi-element chemical analysis, Table 2 details the copper phase analysis, and Fig. 1 illustrates the X-ray Diffractometer (XRD, Empyrean 2, PANalytical, Netherlands) analysis results. Additionally, Table 3 presents the mineral composition of the sample as determined by the Mineral Liberation Analyser (MLA, MLA650, FEI, USA).

Table 1. Multi-element chemical analysis of high-carbon chalcopyrite

Element	Cu	Fe	Pb	Zn	Co	C	S	As
Content(%)	2.50	2.77	0.009	0.008	0.005	6.73	2.27	0.007
Element	MgO	$CaCO_3$	CaF_2	Na_2O	K_2O	TiO_2	Al_2O_3	SiO_2
Content(%)	9.68	25.84	0.88	0.082	2.22	0.32	7.06	31.42

Table 2. Copper phase analysis of high-carbon chalcopyrite

Copper Phase	Primary copper sulfide	Secondary copper sulfide	Free copper oxide	conjunction oxidized copper	Tatol
Content(%)	2.12	0.15	0.02	0.21	2.50
Occupancy(%)	84.80	6.00	0.80	8.40	100.00

Table 1 reveals that the sample predominantly contains copper as the sole valuable element, at 2.50%, with SiO_2 and $CaCO_3$ constituting 31.42% and 25.84% of the gangue, and a total carbon content (C_{total}) of 6.73%. Table 2 demonstrates that the majority of copper in the ore is present as native copper sulfide, constituting 84.80% of the total copper, and the overall distribution rate of copper sulfide is 90.80%. Fig. 1 and Table 3 indicate that chalcopyrite is the primary copper mineral, followed by bornite, with lesser amounts of other sulfide minerals. The gangue minerals mainly consist of dolomite, sericite, and quartz, including a small amount of organic carbon, illustrating that the sample is a high-carbon chalcopyrite.

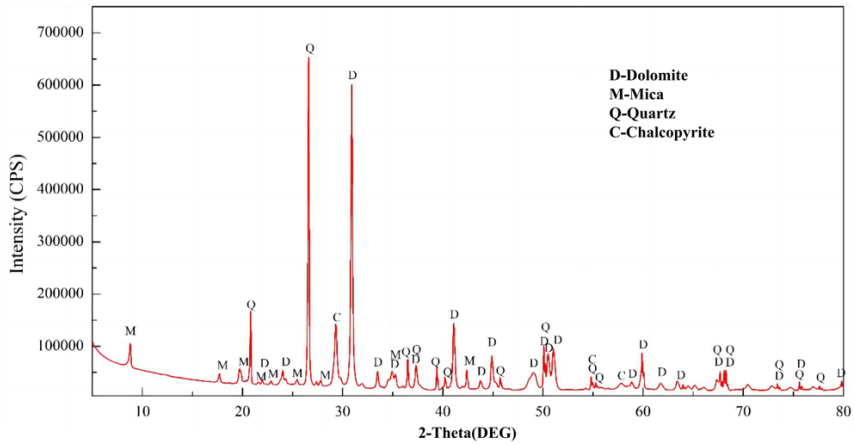

Fig. 1. XRD pattern of high-carbon chalcopyrite

Table 3. Main mineral content of ore

Mineral	chalcopyrite	chalcocite	pyrite	organic carbon	quartz	sericite
Content (%)	5.802	0.151	0.022	2.210	23.022	24.676
Mineral	chlorite	dolomite	serpentine	siderite	rutile	apatite
Content (%)	0.264	41.022	1.742	0.368	0.400	0.221

2.2. Reagents

In chalcopyrite flotation, MIBC (methyl isobutyl carbinol) functions as the frother, Z-200 (O-isopropyl ethylcarbamothioate), PDEC (prop-2-yn-1-yl diethylcarbamodithioate), and Al-DECDT (allyl diethylcarbamodithioate) are employed as collectors. Notably, PDEC, an independently developed

alkyne-based bipolar collector, with its chemical molecular structure is shown in Fig. 2. The remaining chemicals are of industrial grade, manufactured in Qingdao, China.

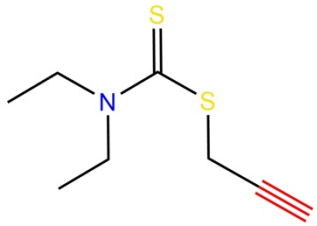

Fig. 2. The molecular structure formula of PDEC

2.3. Experimental method

Single flotation cells (XFD IV0.5L, 0.75L, 1.5L, 3.0L), ball mills (XMQ-Φ240×90, XMQ-Φ150×50), and stirring ball mills (ZJM-150) were utilized for conducting conditional experiments on ore sample feed grinding fineness, collector selection, and middlings regrinding fineness. These experiments established the optimal parameters for the flotation process. Subsequently, the "middlings regrinding flotation process" as shown in Fig. 3, was applied in closed-circuit flotation experiment. To ensure the reliability of the flotation experimental data and conclusions, each group of experiments was conducted in triplicate, and the average value was recorded as the final data.

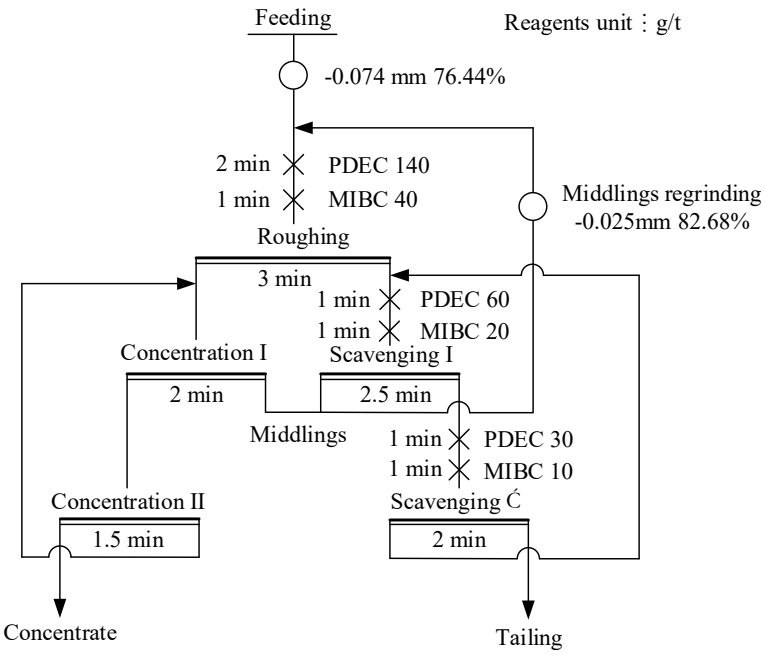

Fig. 3. Flow chart of the closed-circuit flotation experimental process

2.4. DFT model and parameters

In this study, the crystal and surface models of chalcopyrite, along with the molecular model of the collector and their adsorption models, were constructed using Materials Studio 2018, specifically employing its Visualizer and Amorphous cells tools. First-principles calculations were executed in the CASTEP module, encompassing model optimization, calculation of the partial density of states (PDOS), and generation of electron density maps (Chi et al., 2020; Dong et al., 2021; Liu et al., 2022). For chalcopyrite crystal calculations in CASTEP, the optimal generalized gradient approximation (GGA) exchange-correlation function PBE was determined through extensive testing (He et al., 2014). Ultrasoft pseudopotentials facilitated the description of interactions between valence ions and electrons (Chen et al., 2009). System energy and charge density integrations in the brillouin zone utilized a medium scheme for k-point sampling density (Cui and Chen, 2021). The structural model optimization was conducted using the BFGS algorithm, adhering to specific convergence standards: 0.05 eV/Å for interatomic

interaction forces, 0.1 GPa for internal stress within the crystal, 2×10^{-3} Å for maximum atomic displacement, and a self-consistent field convergence precision of 2×10^{-6} eV/atom (Xu et al., 2014; Zhao et al., 2013; Liu et al., 2020; Li et al., 2020).

As shown in Fig. 4, subsequent to the optimization of the chalcopyrite cell, an 8 atomic layers thick chalcopyrite (1 1 2) surface model was developed, fixing the bottom two layers while allowing relaxation for the top six layers. Additionally, a vacuum layer measuring 15 Å was incorporated above this surface.

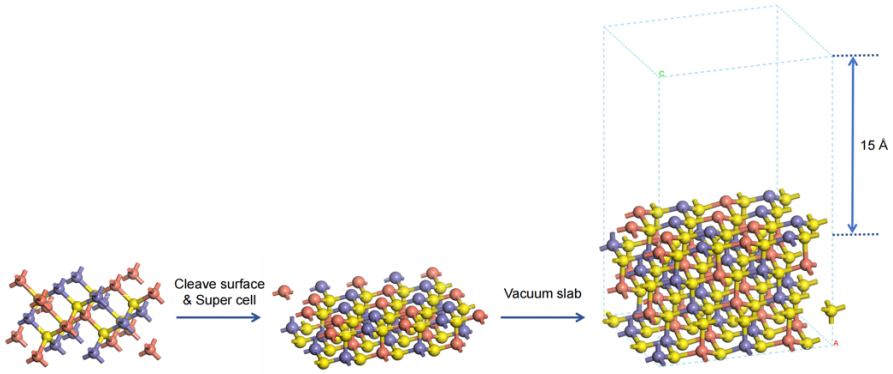

Fig. 4. DFT calculations in the surface model construction process. (where red, blue, yellow, gray, blue, red, white spheres represent Cu, Fe, S, C, N, O, H atoms, respectively)

3. Results and discussion

3.1. Grain size distribution

The grain size distribution of copper minerals in high-carbon chalcopyrite was determined using a Mineral Liberation Analyser (MLA, MLA650, FEI, USA). As detailed in Fig. 5, the distribution is markedly uneven. Copper minerals exceeding 1.28 mm in size comprise 28.53%, those above 0.08 mm constitute 73.91%, and fine-grained minerals less than 0.04 mm represent 16.29%. This data underscores the necessity of fine grinding for the dissociation of these fine-grained minerals. Evidently, implementing staged grinding significantly enhances copper recovery.

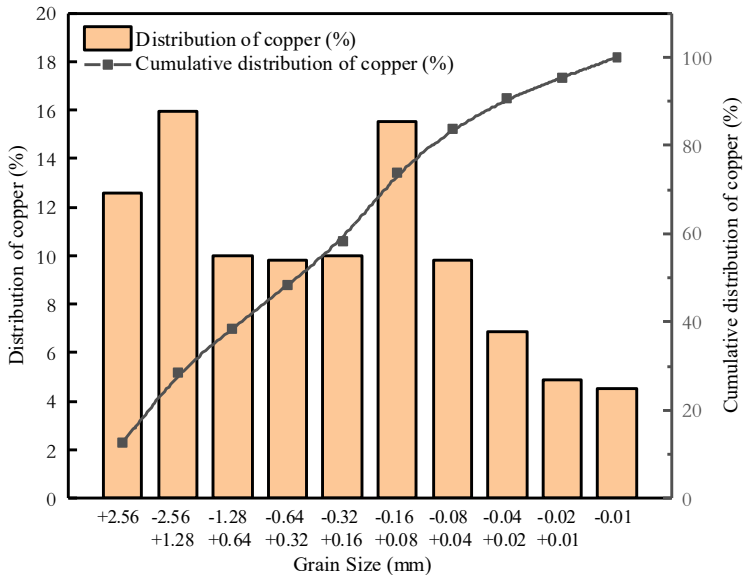

Fig. 5. Grain size distribution of copper minerals

3.2. Microscopic identification

Microscopic examination reveals that the ore-hosting rocks consist predominantly of dolomite and carbonaceous slate. The grain size of chalcopyrite varies considerably, influenced by the disparities between these two rock types and the size of the gaps in both dolomite and carbonaceous slate.

Typically, chalcopyrite is medium to fine-grained, although some copper minerals are found in an ultrafine form. As depicted in Fig. 6 (a), chalcopyrite occupies the fracture cracks within dolomite, presenting irregular granular embedding with notable grain size variation. Fig. 6 (b) illustrates chalcopyrite filling the interlayer gaps, intergranular spaces, or fracture cracks in carbonaceous slate, also with significant grain size variation. Furthermore, the intricate embedding relationship between chalcopyrite and the microfine grains of sericite and quartz, due to their minute size, adds to the complexity, as evidenced in Figs. 6 (c) and 5 (d).

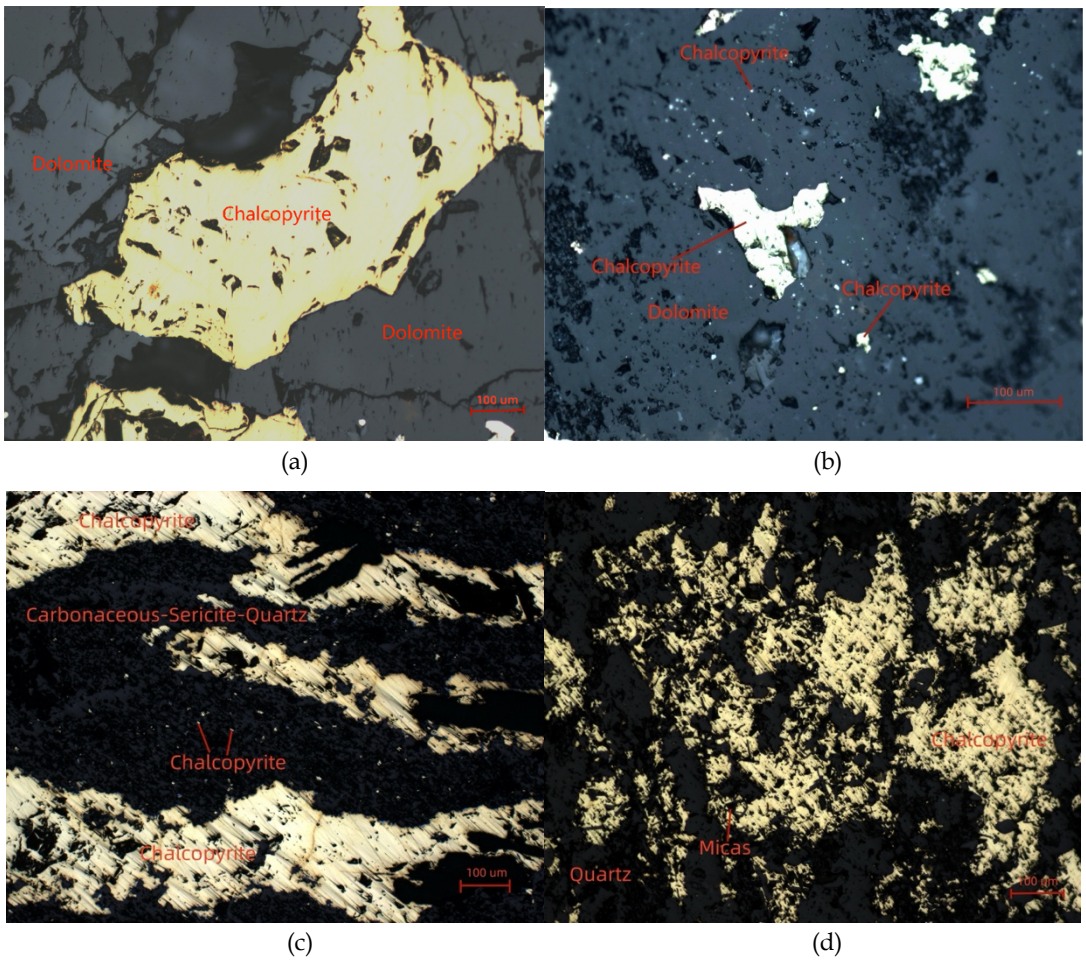

Fig. 6. Microstructure of high-carbon chalcopyrite, (a) chalcopyrite occupies the fracture cracks within dolomite; (b) chalcopyrite filling the dolomite interlayer gaps; (c) carbonaceous-sericite-quartz with the microfine grains of chalcopyrite; (d) halcopyrite with the microfine grains of quartz.

3.3. Grinding fineness

To ascertain the optimal coarse grinding fineness, 1 kg of high-carbon chalcopyrite underwent fine grinding in a cone ball mill (XMQ-Φ240×90). The effects were evaluated through flotation process of one roughing stage, employing 150g/t of Z-200 and 40g/t of MIBC. As depicted in Fig. 7, an increase in grinding fineness led to a gradual rise in the Cu recovery rate, while the Cu grade correspondingly declined. Notably, beyond −0.074 mm grain size content of 76.44%, the enhancement in recovery rate diminished.

Microscopic analysis was conducted to assess the dissociation of copper minerals at an ore −0.074 mm grain size content of 76.44%. Table 4 indicates that at this level of fineness, the dissociation rate of copper minerals was relatively low, at 77.20%. Approximately one-fourth of the copper minerals remained undissociated, predominantly in the form of intergrowths with gangue minerals.

3.4. Collector Selection

The interference from organic carbon in the ore, coupled with the uneven distribution of copper

minerals in high-carbon chalcopyrite, renders the choice of collectors exceedingly important. Thioester collectors, belonging to the non-ionic category, are known for their superior selectivity and efficacy in chalcopyrite collection (Azizi, 2014; Albrecht et al., 2016; Li et al., 2021; Zhang et al., 2022; Zhao et al., 2023). Flotation process of one roughing stage on high-carbon chalcopyrite, with a grinding fineness of −0.074 mm grain size content of 76.44%, employed three thioester collectors: PDEC, Z-200, and Al-DECDT, each with an MIBC dosage of 40g/t. Fig. 8 illustrates that at equivalent dosages, PDEC attained the highest copper grade, while Z-200 and PDEC exhibited comparable copper recovery rates, both surpassing Al-DECDT. Overall, PDEC emerged as the most effective collector in these flotation trials and was used as the collector in subsequent flotation condition experiments.

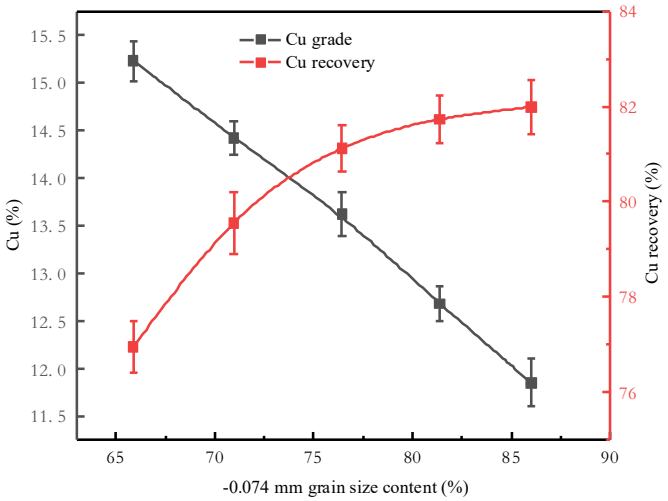

Fig. 7. The influence of grinding fineness

Table 4. Dissociation rate of copper minerals at −0.074 mm grain size content of 76.44%

Grain Size (mm)	Yield (%)	Cu (%)	Dissociation Rate (%)
+0.16	3.66	1.93	17.78
-0.16+0.125	4.47	2.53	29.57
-0.125+0.1	4.16	2.67	48.33
-0.1+0.074	11.27	2.94	59.53
-0.074+0.043	7.97	3.12	63.14
-0.043+0.025	22.28	1.98	76.87
-0.025+0.01	27.35	2.56	96.89
-0.01	18.84	2.56	98.41
Total	100	2.50	77.89

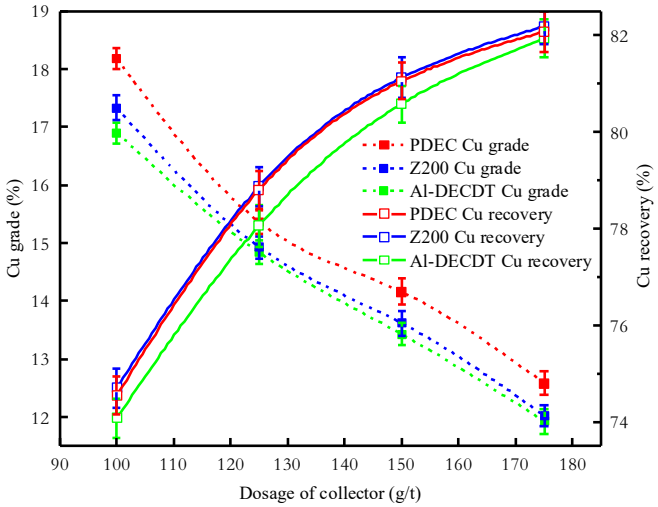

Fig. 8. The influence of collector selection

3.5. Middlings regrinding

In industrial settings, high-carbon chalcopyrite processing typically involves a flotation process of one roughing stage, two cleaning stages, and two scavenging stages. This flotation process was replicated in laboratory conditions, where the middlings were collected. Microscopic examination, as depicted in Fig. 9, reveals the presence of unliberated fine-grained chalcopyrite in both concentration middlings and scavenging concentrates, characterized by their fine size and intergrowth with gangue minerals.

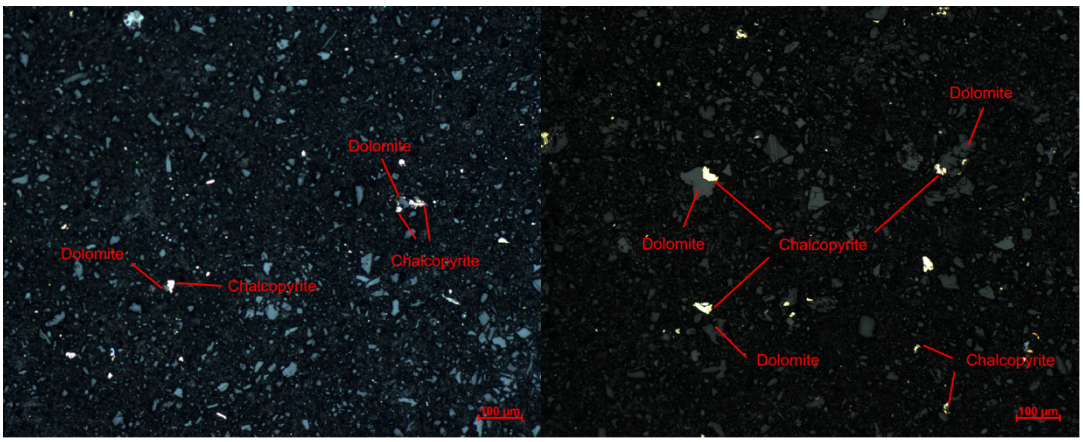

(a) (b)

Fig. 9. Microstructure of middlings, (a) the conjunction of chalcopyrite and dolomite in concentration middlings; (b) the conjunction of chalcopyrite and dolomite in scavenging concentrates

The concentration middlings and scavenging concentrates were amalgamated, resulting in a −0.025 mm grain size content of 40.56% of the sample. This amalgamated sample underwent regrinding in a stirring ball mill (ZJM-150) followed by a flotation process of one roughing, the dosage of PDEC was 120g/t, and MIBC was 30g/t. Fig. 10 demonstrates that as the grinding fineness of the middlings increased, there was an initial rise in the Cu grade and recovery rate, which subsequently declined. Achieving a grinding fineness greater than -0.025 mm, accounting for 80% of the middlings, yielded a copper concentrate with a Cu content exceeding 4% and an operational recovery rate surpassing 70%. These results suggest that fine-grained copper minerals are effectively recoverable through regrinding. In conditions where the grinding fineness exceeds -0.025mm, constituting 85% of the middlings, the pulp becomes rich in fine organic carbon particles and gangue ores, significantly hindering the flotation efficiency for fine-grained chalcopyrite, this disruption leading to an influx of gangue minerals into the copper concentrate, and this effect prominently boosts the yield of the copper concentrate while simultaneously lowering both the copper grade and recovery rate.

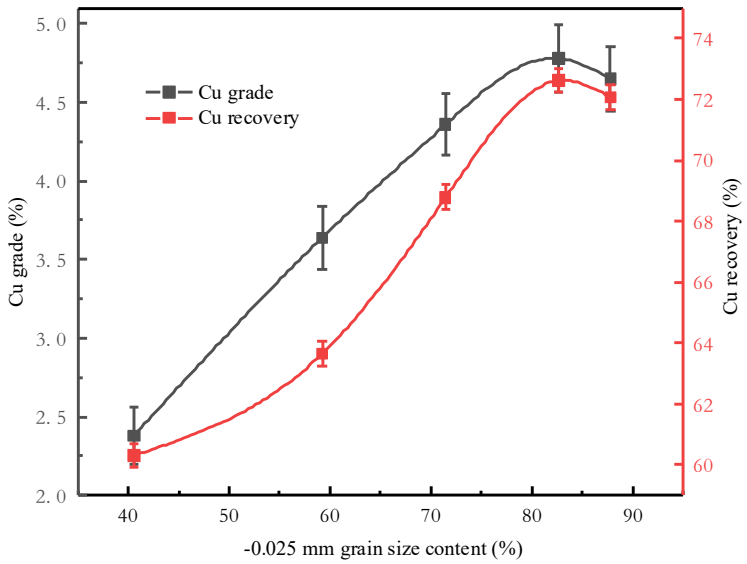

Fig. 10. The influence of middlings regrinding

3.6 Closed-circuit flotation experiment

A closed-circuit flotation experiment was performed to evaluate the effectiveness of the "middlings regrinding" process in enhancing the recovery of high-carbon chalcopyrite. As depicted in Fig. 3, the procedure involved combining and regrinding the cleaning middlings and scavenging concentrate to a fineness of -0.025 mm grain size content of 82.68%, prior to reintroducing them to the roughing stage. In contrast, the conventional flotation process, without "middlings regrinding," involved sequentially returning the cleaning middlings and scavenging concentrate to the preceding stage, maintaining the same experiment parameters as the "middlings regrinding" process. In these closed-circuit experiments, collectors PDEC, Z-200, and Al-DECDT were employed to ascertain the distinctions between "middlings regrinding" and the conventional flotation processes, while also evaluating the efficacy of these collectors in the closed-circuit experiment.

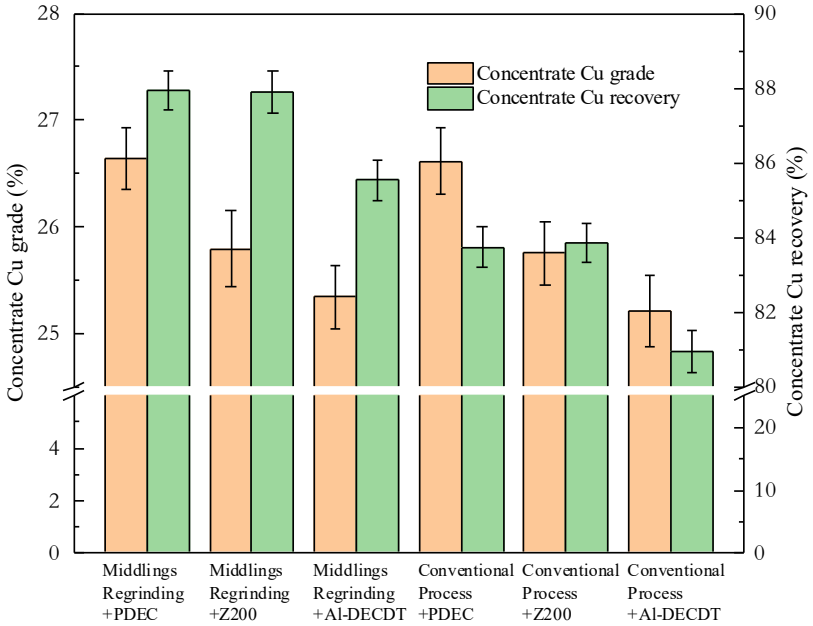

Fig. 11. Comparative closed-circuit flotation experiments with different collector

Fig. 11 demonstrates that processing high-carbon chalcopyrite using the "middlings regrinding" method resulted in a concentrate with a Cu content of 26.79% and a recovery rate of 87.88%. This represents an enhancement of 0.17% in Cu grade and 4.09% in recovery rate compared to the standard process. The "middlings regrinding" approach effectively dissociated the unliberated fine-grained copper minerals and, aided by PDEC, countered the interference from organic carbon, leading to efficient enrichment.

3.7 Density of State Analysis

Analyzing the interaction between the atomic orbitals of PDEC and the chalcopyrite (112) surface contributes to uncovering the chemical interaction forms between PDEC and the chalcopyrite surface (Tkatchenko and Scheffler, 2009; Mishra et al., 2023; Liu et al., 2023). Experimental results have demonstrated that PDEC molecules exhibit their most stable adsorption configuration on the chalcopyrite (112) surface, as shown in Fig. 12. In this configuration, the carbon-sulfur double bond acts as the reaction center. Here, the sulfur atom is adsorbed at an interstitial site between two iron (Fe) atoms on the chalcopyrite (112) surface, and the acetylene group binds to an Fe atom. Fig. 12 elucidates the electronic basis of these bonding interactions, presenting the density of states (DOS) for the sulfur atom in PDEC, its acetylene group, and the corresponding Fe atom on the chalcopyrite surface. The Fermi level is established as the reference zero energy point, and the DOS spectrum ranges from -20 to 10 eV, encapsulating the bonding and antibonding states predominantly of S 3p, C 2p, and Fe 3d.

As indicated in Fig. 13, the S 3p orbit in the carbon-sulfur double bond of PDEC intersects the Fermi level. Before adsorption, this state shows marked localization, but undergoes a shift to lower energy post-adsorption, suggesting enhanced oxidizing properties due to electron loss. Concurrently, the Fe 3d orbit, which forms a bond with S, displays diminished localization. Notably, the S 3p and Fe 3d orbit

undergo hybridization near -2 eV, indicative of a robust interaction between S and Fe atoms, with S partially donating electrons to Fe, thereby establishing a positive coordination bond. In PDEC, the contribution of acetylene to the C 2p orbit near the Fermi level is significant. Initially, this state is highly localized around -2 eV; however, post-adsorption, it shifts toward lower energy, resulting in a marked reduction in the DOS peak and increased delocalization of the C 2p orbit. Moreover, the hybridization between the C 2p and Fe 3d orbit occurs in the -3 to -5 eV range, confirming strong bonding interactions between the acetylene group and the Fe atom.

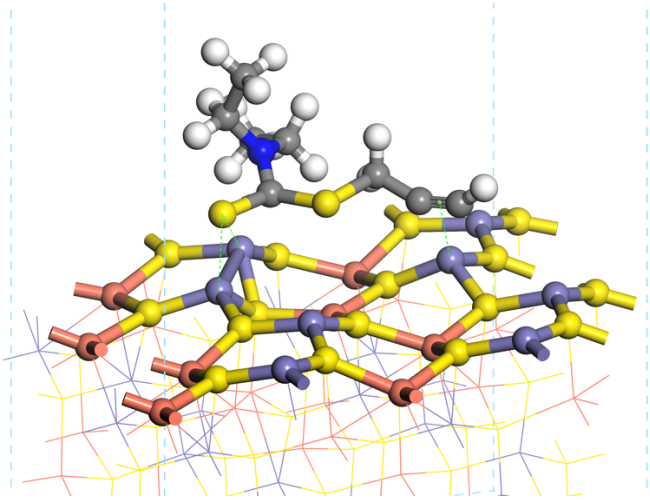

Fig. 12. Adsorption configuration of PDEC on the chalcopyrite (112) surface (where red, blue, yellow, gray, blue, red, white spheres represent Cu, Fe, S, C, N, O, H atoms, respectively)

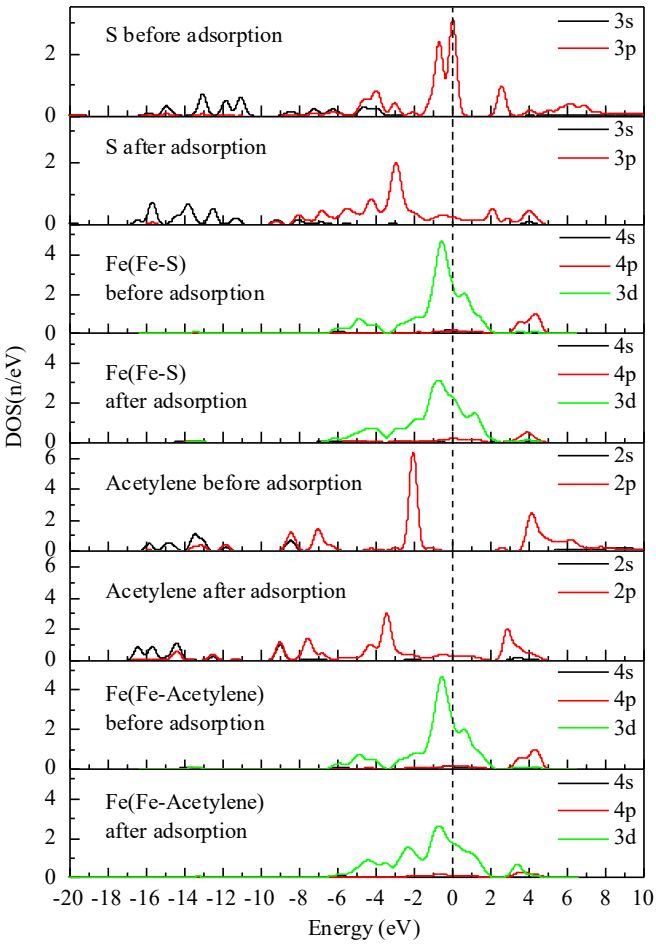

Fig. 13. Density of states between PDEC on the chalcopyrite (1 1 2) surface before and after interaction

4. Conclusions

In this work, we conducted a systematic examination of the ore characteristics of high-carbon chalcopyrite from the DRC, leading to the development of an optimized “middlings regrinding" flotation process aimed at enhancing the recovery of chalcopyrite, informed by process mineralogy findings. Innovatively, we employed an alkyne-based thioester collector, named PDEC, to improve the adsorption of chalcopyrite and mitigate the effects of organic carbon interference. This innovative flotation technique and the use of PDEC as a collector demonstrate considerable potential in facilitating the recovery of similar copper sulfide ores, yielding the subsequent specific conclusions:

(1) The high-carbon chalcopyrite from the DRC, containing 2.50% Cu, with an organic carbon content of 2.210%. The ore is primarily hosted in dolomite and carbonaceous slate. The grain size distribution of chalcopyrite is markedly uneven due to the differences between these rock types, copper minerals exceeding 1.28 mm in size comprise 28.53%, and fine-grained minerals less than 0.04 mm represent 16.29%.

(2) Based on the complexity of chalcopyrite ore, the "middlings regrinding" flotation process effectively dissociated most of the unliberated fine-grained copper minerals, and the application of the PDEC collector in the flotation process yielded a concentrate with a Cu content of 26.79% and a recovery rate of 87.88%. This represents a significant enhancement in chalcopyrite enrichment efficiency, with a 0.17% increase in Cu grade and a 4.09% increase in recovery rate compared to the conventional flotation process.

(3) PDEC demonstrated exceptional selectivity and collection efficiency in chalcopyrite flotation amidst organic carbon interference. Density Functional Theory (DFT) calculations indicated that the S 3p orbit in carbon-sulfur double bond of PDEC and the C 2p orbit in its acetylene group markedly affect its collection capability. This interaction involves hybridization with the Fe 3d orbit on chalcopyrite surface, resonating with corresponding bonding orbitals. During adsorption, the loss of electrons from S atom and the acetylene group leads to a robust bonding interaction with the Fe atoms in chalcopyrite.

The analysis of surface adsorption energy, based on first-principles calculations, was conducted under the theoretical conditions of zero temperature and zero pressure, which often disregards complex variables like surface imperfections, and fluctuations in temperature and pressure. While this approach simplifies the analysis, aiding in the exploration and comprehension of physicochemical principles during flotation, it concurrently narrows the applicability of these findings in practical settings. Future studies should aim for comprehensive analysis utilizing pure samples of chalcopyrite and organic carbon. Moreover, refining first-principles calculations through the incorporation of thermodynamic adjustments and acknowledging surface diversity could lead to a more precise evaluation of the adsorption process in actual situation.

Acknowledgments

This work was financially supported by the Open Project of Yunnan Precious Metals Labo ratory Co., Ltd (YPML-2023050277). Prof. Dongyun Liang (State Key Laboratory of Separation and Comprehensive Utilization of Rare Metal; Institute of Resource Utilization and Rare Earth Development) was acknowledged to provide mineralogical analysis.

References

ZHANG, L., CAI, Z., YANG, J., YUAN, Z., CHEN, Y, 2015. *The future of copper in China – A perspective based on analysis of copper flows and stocks*. Science of the Total Environment, 536, 142-149.

WANG, C., REN., L., MAO, Y., ZHANG., B., SHI, L., 2023. *Analysis of the current distribution status and exploration investment of global copper resources*. China Mining Magazine, 32(S2), 1-6.

SINGER, D.A., 2017. *Future copper resources*. Ore Geology Reviews, 86, 271-279.

KUIPERS, K.J., VAN OERS, L.F., VERBOON, M., VAN DER VOET, E., 2018. *Assessing environmental implications associated with global copper demand and supply scenarios from 2010 to 2050*. Global Environmental Change, 49, 106-115.

MUDD, G.M., JOWITT, S.M., 2018. *Growing global copper resources, reserves and production: Discovery is not the only control on supply*. Economic Geology, 113(6), 1235-1267.

FENG, Q., YANG, W., WEN, S., WANG, H., ZHAO, W., HAN, G., 2022. *Flotation of copper oxide minerals: A review.* International Journal of Mining Science and Technology.

TAHERI B, ABDOLLAHY M, TONKABONI S.Z.S., 2014. *Dual effects of sodium sulfide on the flotation behavior of chalcopyrite:I. Effect of pulp potential.* International Journal of Minerals, Metallurgy, and Materials, 21(5):415-422.

ŠTIRBANOVIĆ, Z., SOKOLOVIĆ, J., MARKOVIĆ, I., ĐORĐIEVSKI, S., 2020. *The effect of degree of liberation on copper recovery from copper-pyrite ore by flotation.* Separation Science and Technology, 55(17), 3260-3273.

PARKER, T., SHI, F., EVANS, C., POWELL, M., 2015. *The effects of electrical comminution on the mineral liberation and surface chemistry of a porphyry copper ore*. Minerals Engineering, 82, 101-106.

ESWARAIAH, C., VENKAT, N., MISHRA, B. K., HOLMES, R., 2015. *A comparative study on a vertical stirred mill agitator design for fine grinding*. Separation Science and Technology, 50(17), 2639-2648.

HASSALL, P., NONNET, E., KEIKKALA, V., KOMMINAHO, T., KOTILA, L., 2016. *Ceramic bead behavior in ultra fine grinding mills*. Minerals Engineering, 98, 232-239.

ZHU, Z.K., YIN, X.W., LIU, L., AN, X.S., ZHANG, C.P., CHENG, W.L., 2019. The New Ultra-fine Grinding Technology and It's Application. Environment, Energy and Earth Sciences, 10.12783/dteees/eece2019/31555

QIU, T., WU, C., AI, G., ZHAO, G., YU, X., 2015. *Effects of multi-stage grinding process and grinding fineness on desulfurization separation of high-sulfurous iron ore.* Procedia engineering, 102, 722-730.

PENG, W., QIU, Y., ZHANG, L., GUAN, J., SONG, S., 2017. *Increasing the fine flaky graphite recovery in flotation via a combined multipletreatments technique of middlings*. Minerals, 7(11), 208.

WAN, H., LU, X., LUUKKANEN, S., QU, J., ZHANG, C., CHEN, Y., BU, X.， 2022. *Properties of flash roasted products from low-grade refractory iron tailings and improvement method for their magnetic separation index*. Physicochemical Problems of Mineral Processing, 58.

YUAN, Z. T., LU, J. W., WU, H. F., LIU, J.T., 2015. *Mineralogical characterization and comprehensive utilization of micro-fine tantalum–niobium ores from Songzi*. Rare metals, 34, 282-290.

WHITEMAN, E., LOTTER, N. O., AMOS, S.R., 2016. *Process mineralogy as a predictive tool for flowsheet design to advance the Kamoa project.* Minerals Engineering, 96, 185-193.

ROY, S., DATTA, A., REHANI, S., 2015. *Flotation of copper sulphide from copper smelter slag using multiple collectors and their mixtures.* International Journal of Mineral Processing, 143, 43-49.

ALBRECHT, T. W. J., ADDAI-MENSAH, J., FORNASIERO, D., 2016. *Critical copper concentration in sphalerite flotation: Effect of temperature and collector.* International Journal of Mineral Processing, 146, 15-22.

AZIZI, A, 2014. *Influence of collector dosage and pulp chemistry on copper flotation*. Geosystem Engineering, 17(6), 311-316.

ZHAO, J., GODIRILWE, L. L., HAGA, K., YAMADA, M., SHIBAYAMA, A, 2023. *Flotation behavior and surface analytical study of synthesized (octylthio) aniline and bis (octylthio) benzene as novel collectors on sulfide minerals.* Minerals Engineering, 204, 108422.

JIANG, T. G., FANG, J. J., ZHANG, T. M., WANG, S., MAO, Y. B, 2014. *The Effect of Different Collectors on Oxidised Copper Ores Flotation.* Advanced Materials Research, 962, 814-817.

ATASHI, H., EBRAHIMIAN, F., 2014. *Investigating the Effects of Different Collectors on Sulfide Minerals Kinetic Flotation of Miduk Copper Mine.* Journal of Advances in Chemistry, 8(3).

MA, Y., YANG, M., TANG, L., ZHENG, S., FU, Y., SHENG, Q., YIN, W, 2022. *Flotation separation mechanism for secondary copper sulfide minerals and pyrite using novel collector ethyl isobutyl xanthogenic acetate*. Colloids and Surfaces A: Physicochemical and Engineering Aspects, 634, 128010.

RYABOY, V. I., SHEPETA, E.D., 2021. *Collector for Copper-Arsenic Ore Flotation*. Gornye nauki i tekhnologii Mining Science and Technology (Russia), 5(4), 297-306.

SOKOLOVIĆ, J., STANOJLOVIĆ, R., ANDRIĆ, L., ŠTIRBANOVIĆ, Z., ĆIRIĆ, N., 2019. *Flotation studies of copper ore Majdanpek to enhance copper recovery and concentrate grade with different collectors.* Journal of Mining and Metallurgy A: Mining, 55(1), 53-65.

LIU, W., MILLER, J. D., SUN, W., HU, Y., 2022. *Analysis of the selective flotation of elemental gold from pyrite using diisobutyl monothiophosphate*. Minerals, 12(10), 1310.

DONG, Z., JIANG, T., XU, B., ZHONG, H., ZHANG, B., LIU, G., YANG, Y., 2021. *Density functional theory study on electronic structure of tetrahedrite and effect of natural impurities on its flotation property.* Minerals Engineering, 169, 106980.

CHI, X., GUO, Y., ZHONG, S., LI, G., LV, X., 2020. *Molecular modelling and synthesis of a new collector O-butyl S-(1-chloroethyl) carbonodithioate for copper sulfide ore and its flotation behavior*. RSC advances, 10(6), 3520-3528.

HE, G. C., JIANG, W., XIANG, H. M., QI, M. C., KANG, Q., 2014. *Density functional theory and its application in mineral processing*. Nonferrous Metals Science & Engineering, 5(2), 62-66.

CHEN, J. H., CHEN, Y., LI, Y.Q., 2009. *DFT calculation of amine cation collectors for zinc oxide flotation*. J. Guangxi Univ., Nat. Sci. Ed, 34, 67-72.

CUI, W., CHEN, J., 2021. *Insight into mineral flotation fundamentals through the DFT method.* International Journal of Mining Science and Technology, 31(6), 983-994.

LIU, G., YANG, X., ZHONG, H, 2017. M*olecular design of flotation collectors: A recent progress.* Advances in Colloid and Interface Science, 246, 181-195.

LI, Y., LIU, Y., CHEN, J., ZHAO, C., 2020. S*tructure-activity of chelating collectors for flotation: A DFT study.* Minerals Engineering, 146, 106133.

ZHAO, G., ZHONG, H., QIU, X., WANG, S., GAO, Y., DAI, Z., HUANG, J., LIU, G, 2013. *The DFT study of cyclohexyl hydroxamic acid as a collector in scheelite flotation.* Minerals engineering, 49, 54-60.

XU H., ZHONG H., WANG, S., 2014. *Synthesis of 2-ethyl-2-hexenal oxime and its flotation performance for copper ore.* Minerals Engineering,66-68.

ZHANG, L.G., OUYANG, C.Z., LI, W.F., 2022. New Flotation Collector CYC-20 for Beneficiation of Associated Copper Minerals from a Shandong Iron Mine. Mining and Metallurgical Engineering, 42(2),70-72.

LI, D., DAI, X. R., LI, S.N., 2021. E*xperimental Study on Recovery of Mirador Copper Minerals by Asynchronous Flotation Process*. Modern Mning, 37(07):112-115+143.

TKATCHENKO, A., SCHEFFLER, M, 2009. *Accurate Molecular Van Der Waals Interactions from Ground-State Electron Density and Free-Atom Reference Data.* J. Phys. Rev. Lett, 102, 073005.

MISHRA, S., PANDA, S., AKCIL, A., DEMBELE, S, 2023. *Biotechnological avenues in mineral processing: Fundamentals, applications and advances in bioleaching and bio-beneficiation*. Mineral Processing and Extractive Metallurgy Review, 44(1), 22-51.

LIU, Y., CHEN, J., LI, Y., ZHAO, C., 2023. *First-principles study on the co-adsorption of water and oxygen molecules on chalcopyrite (112)-M surface*. International Journal of Mining Science and Technology, 33(8), 1055-1063.